

Well test mathematical model of multi-stage fracturing horizontal well for deep layer shale gas

JIN PANG², DI LUO³, SHANG LI⁴, HONG LIU², JIE
LIANG², DONGMEI JIANG²

Abstract. The well test model of multi-stage fracturing horizontal well in shale gas reservoir plays an important role in studying the seepage characteristics of shale gas and evaluating the completion effect. Firstly, a physical model of shale gas multi-stage fracturing horizontal well is established based on the geological and production characteristics of deep shale gas reservoirs. Then, the seepage model in the natural fracture system of shale gas reservoir is established based on the physical model, and the model is processed by dimensionless, perturbation transformation and Laplace transformation. The simplified zero-order model is obtained. Next the shale gas migration model in the matrix is established according to the desorption characteristics of micro-nano-matrix porosity. And then according to the idea of Huiyuan function method, after the basic solution of the unstable seepage flow model in the production of a vertical line in the shale gas reservoirs obtained, the artificial fracture joints are discretized by element along the fracture paths, and the pressure response of each discrete element is obtained with the basis of the obtained line of the basic solution along the discrete fracture unit integration, and the equations are connected to obtain a multi-order matrix, the pressure response caused by the multi-stage fracturing horizontal well can be obtained after solve the matrix. Finally, Stehfest numerical inversion and Gaussian elimination are used to draw the typical curve of bottom pressure of multi-stage fracturing horizontal wells in shale gas reservoir, The seepage mechanism and the sensitivity of curve parameters are analyzed according to the typical curve.

Key words. Shale gas, multi-stage fracturing, horizontal well, well test model, deep layer, pressure dynamics.

¹Acknowledgment - Chongqing basic science and frontier technology research project(cst.c2016jcyjA0745); Chongqing education commission science and technology research project(KJ1601322)

²Workshop 1 - Chongqing University of Science and Technology

³Workshop 2 - Southwest Oil and Gas Field Branch Shunan Gas Mine

⁴Workshop 3 - Zhejiang Oilfield Branch Southwest Gas Production Plant

1. Introduction

The study of shale gas well seepage mathematical model began in the 1980s, early scholars mainly consider the development of natural fractures in shale gas reservoirs, based on the classic Warren-Root dual-hole model, adsorption and desorption are coupled into the model to achieve the description of the law of shale gas migration, but almost never consider the diffusion within matrix pores, such as Kucuk et al [1]. Kuuskraa [2] studied the effect of the presence of adsorbed gas on the recovery of shale gas reservoirs and pointed out the importance of adsorbed gas in the development of shale gas. Ozkan et al. [3-5] studied the percolation of shale gas using a two-hole media model, assuming that shale gas flow in natural fractures for Darcy flow, considering the mechanism of diffusion migration in the matrix at the same time, a model of shale fracture and matrix coupling was established, but the model does not take the existence of desorption in the shale matrix and non-Darcy flow phenomenon into consideration. Wu et al.[6] considered the flow of shale gas in the matrix as a non-Darcy flow with a slip-page effect, the flow in natural fractures is high-speed non-Darcy flow, a seepage model was established to study the seepage law of shale gas, but the seepage model did not consider the unique desorption and diffusion mechanism during the development of shale gas reservoirs. Rasheed and Robert [7] studied the production dynamics of multistage fracturing horizontal wells in shale gas reservoirs, but also neglected the effects of desorption and diffusion during the development of shale gas reservoirs. In addition, the shale gas accumulation mechanism, seepage and well test theory Had been studied [8-12] by so many scholars, but there are still many deficiencies. In general, shale gas well testing theory is not mature, especially for deep layer shale gas reservoirs, there are more defects. Therefore, in order to get a reliable explanation of the results, it is necessary to establish a well test interpretation model which accords with the characteristics of shale gas reservoirs from the actual situation of geological and seepage characteristics of deep layer shale gas reservoirs.

2. Physical model

In the shale gas reservoir, a horizontal well is formed by M strips fractures after multi-stage hydraulic fracturing, the y -axis coordinate of the intersection of the intersecting fracture of the i ($1 \leq i \leq M$) and the y -axis is y_i . The other assumptions are as follows:

- (1) There are natural fractures and micro-nano-matrix pores in the reservoir;
- (2) The flow in the natural fracture system is a single-phase Darcy isothermal seepage, and there is a stress-sensitive effect, while the fluid in the micro-nano-matrix pores can only diffuse into the natural cracks under the effect of concentration difference;
- (3) There is a constant gas production q_{sc} in the multi-stage fracturing horizontal well;
- (4) Gravity and capillary force are ignored;
- (5) Reservoir initial formation pressure is p_i ;

(6) Due to the control of the ground stress, the fracturing fractures may not be perpendicular to the horizontal well, but to a certain angle with horizontal well.

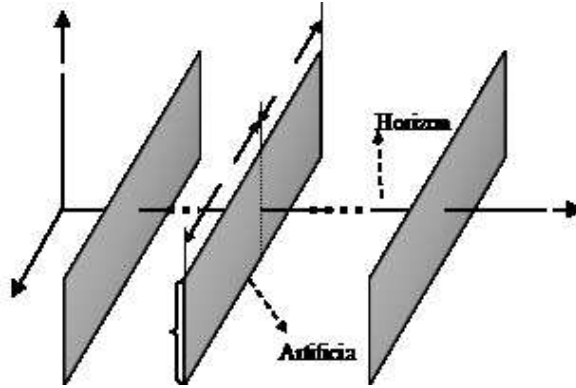


Fig. 1. Physical model of fracturing horizontal wells with multi-stage fracturing

3. Seepage model within natural fractures

3.1. Differential equation of seepage flow

The seepage differential equation within the natural fracture system of shale gas reservoir, which is as formula (1) shows:

$$\frac{\partial^2 \psi}{\partial r^2} + \frac{1}{r} \frac{\partial \psi}{\partial r} + \beta \left(\frac{\partial \psi}{\partial r} \right)^2 = e^{(\psi_i - \psi)\beta} \left(\frac{\phi \mu_i C_{gi}}{k_i} \frac{\partial \psi}{\partial t} + \frac{2p_{sc} T}{k_i T_{sc}} \frac{\partial V}{\partial t} \right) \quad (1)$$

3.2. Fixed solution condition

Line inner boundary condition:

$$\lim_{\varepsilon \rightarrow 0} e^{-(\psi_i - \psi)\beta} r \frac{\partial \psi}{\partial r} \Big|_{r=\varepsilon} = \frac{p_{sc} \widehat{q}(t) T}{\pi k h T_{sc}} \quad (2)$$

External boundary condition:

$$\psi|_{r \rightarrow \infty} = \psi_i \quad (3)$$

Initial condition:

$$\psi|_{t=0} = \psi_i \quad (4)$$

The seepage model within the natural fracture system of shale gas reservoir consists of formula (1) ~ (4).

3.3. Dimensionless model

The dimensionless parameters of the model are shown in Table 1.

According to the parameters defined in Table 1, the equations (1) to (4) become dimensionless:

$$\frac{\partial^2 \psi_D}{\partial r_D^2} + \frac{1}{r_D} \frac{\partial \psi_D}{\partial r_D} - \gamma_D \left(\frac{\partial \psi_D}{\partial r_D} \right)^2 = e^{\gamma_D \psi_D} \left[\omega \frac{\partial \psi_D}{\partial t_D} + (1 - \omega) \frac{\partial V_D}{\partial t_D} \right] \quad (5)$$

$$\lim_{\varepsilon_D \rightarrow 0} e^{-\psi_D \gamma_D} r_D \frac{\partial \psi_D}{\partial r_D} \Big|_{r=\varepsilon_D} = -\hat{q}_D \quad (6)$$

$$M_{pq} = \int \int x^p y^q f(x, y) dx dy \quad p, q = 0, 1, 2, \dots \quad (7)$$

$$F_{pq} = \int \int f(r, \theta) g_p(r) e^{jq\theta} r dr d\theta \quad (8)$$

The formula (5) ~ (8) is the dimensionless mathematical model of the unstable seepage flow within the natural fracture system of the shale gas reservoir.

Table 1. Dimensionless parameter definition table λ for a trapezoidal plate for different values of taper constant β_1 and constant aspect ratios $a/b = 1.0$, $c/b = 0.5$

Dimensionless variable	expression
Pseudo pressure difference (Ψ)	$\Delta\psi = \psi_i - \psi$
Dimensionless pseudo pressure (Ψ_D)	$\psi_D = \frac{\pi k_i h T_{sc}}{p_{sc} q_{sc} T} \Delta\psi$
Dimensionless radial distance (r_D)	$r_D = \frac{r}{L_{ref}}$
Variation of free gas concentration in bedrock (V_D)	$V_D = V_i - V$
Total system capacity of elastic storage (Λ)	$\Lambda = \phi C_{gi} + \frac{2\pi k_i h}{q_{sc} \mu_i}$
Dimensionless time (t_D)	$t_D = \frac{k_i t}{\mu_i \Lambda L_{ref}^2}$
Elastic volume ratio (ω)	$\omega = \frac{\phi C_{gi}}{\Lambda}$
Dimensionless permeability modulus (γ_D)	$\gamma_D = \beta \frac{p_{sc} q_{sc} T}{\pi k_i h T_{sc}}$
Linear dimensionless yield \hat{q}_D	$\hat{q}_D = \hat{q}_D(t_D) = \hat{q}(t)/q_{sc}$

3.4. Perturbation transformation and Laplace transformation

The Pedrosa transform formula is introduced into formula (9):

$$\psi_D(r_D, t_D) = -\frac{1}{\gamma_D} \ln [1 - \gamma_D \xi_D(r_D, t_D)] \quad (9)$$

The model of natural fracture seepage described by formula (5) ~ (8) turns into formula (10) ~ (13):

$$\frac{\partial^2 \xi_D}{\partial r_D^2} + \frac{1}{r_D} \frac{\partial \xi_D}{\partial r_D} = [1 - \gamma_D \xi_D] \left\{ \omega \frac{\partial \xi_D}{\partial t_D} + (1 - \omega) \left[(1 - \gamma_D \xi_D) \frac{\partial V_D}{\partial t_D} \right] \right\} \quad (10)$$

$$\lim_{\varepsilon_D \rightarrow 0} r_D \frac{\partial \xi_D}{\partial r_D} \Big|_{r_D = \varepsilon_D} = -\widehat{q}_D \quad (11)$$

$$\|F_{pq}^{rotated}\| = \sqrt{F_{pq}^{rotated} \times (F_{pq}^{rotated})^*} = \|F_{pq}\| \quad (12)$$

$$F_{pq} = \int s_q(r) g_p(r) r dr \quad (13)$$

The perturbation transformation formula is introduced

$$\xi_D = \xi_{D0} + \gamma_D \xi_{D1} + \gamma_D^2 \xi_{D2} + O(\gamma_D^3) \quad (14a)$$

$$-\frac{1}{\gamma_D} \ln[1 - \gamma_D \xi_D(r_D, t_D)] = \xi_D(r_D, t_D) + \frac{1}{2} \gamma_D \xi_D^2(r_D, t_D) + O(\gamma_D^2) \quad (14b)$$

Considering the dimensionless permeability modulus γ_D is very small, the precision can be satisfied by taking the perturbation solution of zero order, so there are:

$$\frac{\partial^2 \xi_{D0}}{\partial r_D^2} + \frac{1}{r_D} \frac{\partial \xi_{D0}}{\partial r_D} = \omega \frac{\partial \xi_{D0}}{\partial t_D} + (1 - \omega) \frac{\partial V_D}{\partial t_D} \quad (14)$$

$$\lim_{\varepsilon_D \rightarrow 0} r_D \frac{\partial \xi_{D0}}{\partial r_D} \Big|_{r_D = \varepsilon_D} = -\widehat{q}_D \quad (15)$$

$$\xi_{D0} \Big|_{r_D \rightarrow \infty} = 0 \quad (16)$$

$$\xi_{D0} \Big|_{t_D \rightarrow \infty} = 0 \quad (17)$$

Then, the Lapalace transform based on t_D is introduced:

$$\overline{\xi_{D0}} = \int_0^{+\infty} \xi_{D0} e^{-st_D} dt_D \quad (18)$$

$$\overline{V_D} = \int_0^{+\infty} V_D e^{-st_D} dt_D \quad (19)$$

The formula (15) ~ (18) becomes:

$$\frac{d^2 \overline{\xi_{D0}}}{dr_D^2} + \frac{1}{r_D} \frac{d \overline{\xi_{D0}}}{dr_D} = \omega s \overline{\xi_{D0}} + (1 - \omega) s \overline{V_D} \quad (20)$$

$$\lim_{\varepsilon_D \rightarrow 0} \frac{d \overline{\xi_{D0}}}{dr_D} \Big|_{r_D = \varepsilon_D} = -\overline{\widehat{q}_D} \quad (21)$$

$$\overline{\xi_{D0}}|_{r_D \rightarrow \infty} = 0 \quad (22)$$

The formula (22) ~ (23) is the zero-order model of the unsteady seepage flow model within the natural fracture system of the shale gas reservoir by Laplace transformation and perturbation.

4. Migration model within the matrix

There are a large number of micro-nano-pores in the matrix of shale, the size of these pores is minimal, the specific surface ratio is large, which cause a large amount of shale gas is adsorbed on the surface of the pores, when the pressure drops, the gas will be desorbed from the adsorption state and turned into free gas. Due to the pore size is very small, and the permeability is extremely low, therefore, the prevailing view is that the shale gas in the matrix pores could not flow into the natural fracture system through the seepage flow under the action of the pressure difference, but it can flow into the fractures through diffusion with the effect of concentration difference, this diffusion phenomenon can be described by Fick's law.

$$\frac{\partial V}{\partial t} = \frac{6D\pi^2}{R_m^2}(V_E - V) \quad (23)$$

In combination with the definition of V_D in Table 1, and order: $V_{ED} = V_i - V_E$, $\lambda = \frac{\mu_i \Lambda L_{ref}^2}{k_i \tau}$, $\tau = \frac{R_m^2}{6D\pi^2}$

So the formula (24) can be turned into formula (25):

$$\frac{\partial V_D}{\partial t_D} = \lambda(V_{ED} - V_D) \quad (24)$$

For the quasi-steady-state diffusion case, based on the Langmuir isothermal adsorption theory, equations (26) and (27) can be obtained:

$$V_E = V_L \frac{\psi}{\psi_L + \psi} \quad (25)$$

$$V_i = V_L \frac{\psi_i}{\psi_L + \psi_i} \quad (26)$$

Based on the definition of formula V_{ED} , and formula (26) and (27), formula (28) can be obtained:

$$V_{ED} = V_i - V_E = \sigma \psi_D \quad (27)$$

In the formula (28), σ is the adsorption index, and its expression is formula (29a):

$$\sigma = \frac{p_{sc} q_{sc} T}{\pi k h T_{sc}} \frac{\psi_L V_L}{(\psi_L + \psi)[\psi_L + \psi_i]} \quad (29a)$$

Within the range of general pressure changes, it can be assumed that σ is a constant, when $\psi = \psi_i$, formula (29a) is simplified and turned into formula (29b):

$$\sigma = \frac{p_{sc} q_{sc} T}{\pi k h T_{sc}} \frac{\psi_L V_L}{(\psi_L + \psi_i)[\psi_L + \psi_i]} \quad (29b)$$

The Laplace transform of equation (25) and (??)26) is performed,

$$s\overline{V_D} = \lambda (\overline{V_{ED}} - \overline{V_D}) \quad (28)$$

$$\overline{V_{ED}} = \sigma\overline{\psi_D} \quad (29)$$

Simultaneous formulas (30) and (??)31), formula (32) can be obtained:

$$\overline{V_D} = \frac{\sigma\lambda}{s + \lambda} \overline{\psi_D} \quad (30)$$

5. Coupling of seepage model and diffusion model

Substituting formula (32) into formula (21); the formula (33) can be obtained:

$$\frac{d^2\overline{\xi_{D0}}}{dr_D^2} + \frac{1}{r_D} \frac{d\overline{\xi_{D0}}}{dr_D} = \omega s\overline{\xi_{D0}} + \frac{\sigma\lambda(1-\omega)}{s+\lambda} \overline{s\psi_D} \quad (31)$$

Taking use of perturbation transformation formula (14a) and (14b), considering that the dimensionless permeability modulus is small, zero order perturbation solution can meet the precision, and based on the formula (33), the formula (34) can be obtained:

$$\frac{d^2\overline{\xi_{D0}}}{dr_D^2} + \frac{1}{r_D} \frac{d\overline{\xi_{D0}}}{dr_D} = \omega s\overline{\xi_{D0}} + \frac{\sigma\lambda(1-\omega)}{s+\lambda} \overline{s\xi_{D0}} \quad (32)$$

Order:

$$f(s) = \omega s + \frac{\sigma\lambda(1-\omega)}{s+\lambda} s \quad (33)$$

So the formula (34) can be turned into formula (36):

$$\frac{d^2\overline{\xi_{D0}}}{dr_D^2} + \frac{1}{r_D} \frac{d\overline{\xi_{D0}}}{dr_D} = f(s)\overline{\xi_{D0}} \quad (34)$$

The formula (36) is the differential equation which is coupled between thenatural fractured seepage differential equation and the quasi-steady-state differential equation of the matrix, the general solution is equation (37):

$$\overline{\xi_{D0}} = AK_0 \left(\sqrt{f(s)}r_D \right) + BI_0 \left(\sqrt{f(s)}r_D \right) \quad (35)$$

From the properties of the Bessel function, it is necessary to have $B = 0$ for the formula (23) is established in the fracture model, so the formula (37) can be turned into formula (38):

$$\overline{\xi_{D0}} = AK_0 \left(\sqrt{f(s)}r_D \right) \quad (36)$$

Formula (38) is introduced into the formula (22) of the fractured model, formula (39) can be obtained:

$$A \left[-\sqrt{f(s)r_D} \right] K_1 \left(\sqrt{f(s)r_D} \right) \Big|_{r_D \rightarrow 0} = -\bar{q}_D \tag{37}$$

From the formula (39) and the Bessel function $xK_1(x)|_{x \rightarrow 0} = 1$, formula (40) can be obtained:

$$A = \bar{q}_D \tag{38}$$

Formula (40) is introduced into the formula (38), formula (41) can be obtained:

$$\bar{\xi}_{D0} = \bar{q}_D K_0 \left(\sqrt{f(s)r_D} \right) \tag{39}$$

Formula (41) is the basic solution of the zero-order perturbation obtained by coupling the natural fracture seepage model with the quasi-steady-state diffusion model.

6. Unstable pressure dynamics

6.1. Pressure response

Considering that the dimensionless permeability modulus γ_D is very small, zero order perturbation solution can meet the precision, therefore, the formula (41) is written directly as formula (42):

$$\bar{\xi}_D = \bar{q}_D K_0 \left(\sqrt{f(s)r_D} \right) \tag{40}$$

Using the definition in Table 1, the formula (42) can be written as formula (43):

$$\bar{\xi}_D = \frac{\bar{q}}{q_{sc}} K_0 \left(\sqrt{f(s)r_D} \right) \tag{41}$$

If the line is not located in the gas reservoir center, but in any position (x_w, y_w) , the formula (43) can be written as formula (44):

$$\bar{\xi}_D = \frac{\bar{q}}{q_{sc}} K_0 \left(\sqrt{f(s)R_D} \right) \tag{42}$$

And among them:

$$g_p^{Zerinke}(r) = \sum_{s=0}^{(p-|q|)/2} (-1)^s \times \frac{(p-s)!}{s! \left(\frac{p+|q|}{2} - s\right)! \left(\frac{p-|q|}{2} - s\right)!} r^{p/2-s}$$

Although the total surface gas production volume of the fractured horizontal well is constant, the flow of the formation into the each crack is not always equal throughout the flow process, even for different parts of the same crack, the flow from the formation is not always equal, the method of unit dispersion is adopted here for

this kind of flow inhomogeneity problem.

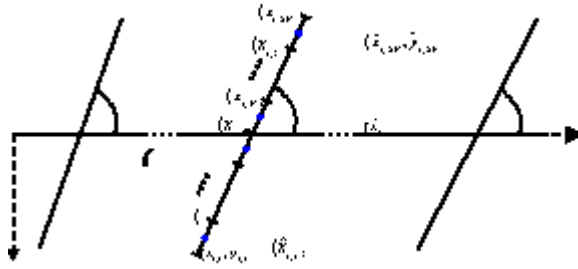


Fig. 2. the discrete diagram of multi-stage fracturing horizontal well unit

As is shown in Fig 2, the left and right wings of each fracture are equally divided into N discrete units, so there are 2N discrete units on each fracture, according to the geometric relationship, the midpoint (nodal) coordinates of the jth discrete element on the ith crack are denoted as formula (45) and (46):

When 1 j N: Formula (45) can be obtained:

$$\left(\frac{2j - 2N - 1}{2N} X_{fLi} \sin \alpha_i, y_i + \frac{2N - 2j + 1}{2N} X_{fLi} \cos \alpha_i \right) \quad (43)$$

When N + 1 j 2N: Formula (46) can be obtained:

$$\left(\frac{2N + 2j - 1}{2N} X_{fRi} \sin \alpha_i, y_i + \frac{2N - 2j + 1}{2N} X_{fRi} \cos \alpha_i \right) \quad (44)$$

According to the geometric relationship, the coordinates of the jth end point on the ith fracture are denoted as formulas (47) and (48):

When 1 j N: Formula (47) can be obtained:

$$\left(\frac{j - N - 1}{N} X_{fLi} \sin \alpha_i, y_i + \frac{N - j + 1}{N} X_{fLi} \cos \alpha_i \right) \quad (45)$$

When N + 1 j 2N: Formula (48) can be obtained:

$$\left(\frac{2j - N - 1}{N} X_{fRi} \sin \alpha_i, y_i + \frac{N - j + 1}{N} X_{fRi} \cos \alpha_i \right) \quad (46)$$

$$\Delta y_i = y_i - y_{i-1} \quad (47)$$

The straight line equation of the ith fracture is equation (50):

$$y_{wi} = -\text{ctg}(\alpha_i)x_{wi} + y_i \quad (48)$$

After dimensionless:

$$y_{wDi} = -\text{ctg}(\alpha_i)x_{wDi} + y_{Di} \quad (49)$$

And among them:

$$\psi_{ab}(r) = \frac{1}{\sqrt{b}} \psi\left(\frac{r-b}{a}\right)$$

Assuming that the linear density flow q_{ij} on the same discrete fracture element is equal, so the response of the j th discrete unit on the i th fracture to the point (x_D, y_D) , which can be obtained by integrating on the unit with the line basic solution formula (44):

$$\overline{\xi_{D i, j}}(x_D, y_D) = \frac{\bar{q}_{i, j}(u)}{q_{sc}} \int_{\Gamma_{i, j}} K_0 \left[\sqrt{f(s)} R_D(x_D, y_D; x_{wD}, y_{wD}) \right] dl \quad (50)$$

And among them: $R_D(x_D, y_D; x_{wD}, y_{wD}) = \sqrt{(x_D - x_{wD})^2 + (y_D - y_{wD})^2}$

$$dl = \sqrt{dx^2 + dy^2}$$

Taking use of the formulas (50) and (51), the curve integral of formula (52) is transformed into a single integral of x_{wi} :

$$q_{D i, j}(u) = \frac{q_{i, j}(u) L_{ref}}{q_{sc}} \quad (51)$$

And among them:

$$R_D(x_D, y_D; x_{wD i}) = \sqrt{(x_D - x_{wD i})^2 + [y_D + \text{ctg}(\alpha_i) x_{wD i} - y_{D i}]^2} \quad (52)$$

According to the superposition principle of potential, the response of the $2N \times M$ discrete units on the M vertical cracks at any point on the plane (x_D, y_D) is formula (57):

$$\overline{\xi_D}(x_D, y_D) = \sum_{i=1}^M \sum_{j=1}^{2N} \overline{\xi_{D i, j}}(x_D, y_D) \quad (53)$$

If (x_D, y_D) is taken as the node $(\hat{x}_{Dk, v}, \hat{y}_{Dk, v})$ of the discrete unit $(1 \text{ K M}, 1 \text{ v } 2N)$, then the formula (58) can be obtained:

$$\overline{\xi_D}(\hat{x}_{Dk, v}, \hat{y}_{Dk, v}) = \sum_{i=1}^M \sum_{j=1}^{2N} \overline{\xi_{D i, j}}(\hat{x}_{Dk, v}, \hat{y}_{Dk, v}) \quad (54)$$

In low permeability shale gas reservoirs, the permeability of the gas reservoir is much smaller than that of the artificial fracture, so the seepage resistance of the fluid in the artificial fracture is much smaller than the seepage resistance in the formation, therefore, the artificial fracture can be regarded as an infinite diversion fracture, that is to say, we can ignore the pressure loss of the fluid generated in the artificial fracture, then formula (59) can be obtained:

$$\overline{\xi_D}(\hat{x}_{Dk, v}, \hat{y}_{Dk, v}) = \overline{\xi_{wD}} \quad (55)$$

So formula (58) can be turned into formula (60):

$$\overline{\xi_{wD}} = \sum_{i=1}^M \sum_{j=1}^{2N} \overline{\xi_{Di,j}} (\hat{x}_{Dk,v}, \hat{y}_{Dk,v}) \quad (56)$$

Taking different $k, v(k=1, 2, \dots, M; v=1, 2, \dots, 2N)$ in formula (60), $2N \times M$ equations can be obtained, the uncertain $\overline{q_{Di,j}}(u)$ and $\overline{\xi_{wD}}$ that need to be solved are total $2N \times M + 1$, an equation is still needed, total production conditions of fracturing horizontal wells should also be used:

$$\sum_{i=1}^M \sum_{j=1}^{2N} [\overline{q_{i,j}} \Delta L_{fi,j}] = \frac{q_{sc}}{u} \quad (57)$$

$\Delta L_{fi,j}$ is the length of the unit (i, j), and then formula (61) can be turned into formula (62):

$$\sum_{i=1}^M \sum_{j=1}^{2N} [\overline{q_{Di,j}} \Delta L_{fDi,j}] = \frac{1}{u} \quad (58)$$

Formulas (60) and (62) represent $2N \times M + 1$ linear algebraic equation, the uncertain $\overline{q_{Di,j}}(u)$ and $\overline{\xi_{wD}}$ are total $2N \times M + 1$, thus it can be closed to solve. It can be expressed in matrix form:

$$AX = C \quad (59)$$

The integrals in the coefficient matrix can be calculated by using numerical integrals. Since the matrix is a dense matrix, therefore, the direct solution (e.g. Gauss elimination) of linear algebraic equations can be used to solve the matrix, and it is not necessary for an iterative solution (such as Jacobi iterations, Gaussian-Saide iterations, etc.).

6.2. Typical Curve and Sensitivity Analysis

Through programming, Stehfest numerical inversion and Gaussian elimination are used to draw the typical curve of bottom pressure of multi-stage fracturing horizontal well in shale gas reservoirs, Fig.2 shows the effect of different parameters on the typical curve when using a quasi-steady-state diffusion model to calculate.

The seepage process of fracturing horizontal well in shale gas reservoir can be divided into nine stages: Early pure wellbore storage section, the pressure and pressure derivative of this section is a straightline with a slope of 1; The transition section after early pure wellbore storage section, the pressure derivative curve of this section is a "hump"; The first linear flow section, the pressure derivative curve of this section is a straight line with a slope of 0.5; The transition section which is from the initial linear flow to the initial quasi-radial flow; The initial quasi-radial flow section around each artificial fracture, the ordinate value of the pressure derivative is "1/M" in this section; The second linear flow section; The transition section be-

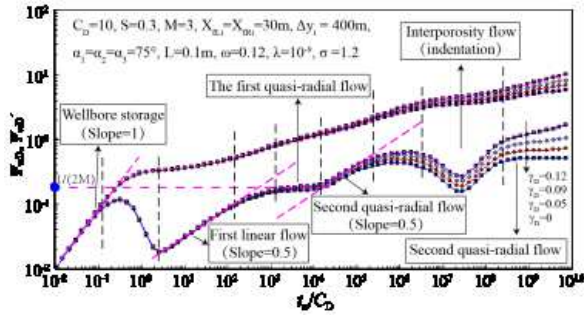


Fig. 3. The typical curve of different γ_D

tween the second linear flow section and the channeling section; Channeling section, this section mainly reflects the flow of the matrix flowing to the fracture, the pressure derivative curve shows a downward "depression"; Late quasi-radial flow section, when " $\gamma_D = 0$ ", the section is a horizontal line with an ordinate value of "0.5", with γ_D gradually increasing, the section is a straight line with increasing slope, which reflecting the stronger the degree of stress sensitivity, the later energy consumption is faster. Fig.4 shows the effect of the elastic storage ratio ω on the typical curve. As it can be seen from the Fig, when the ω is much smaller, the depression is much deeper.

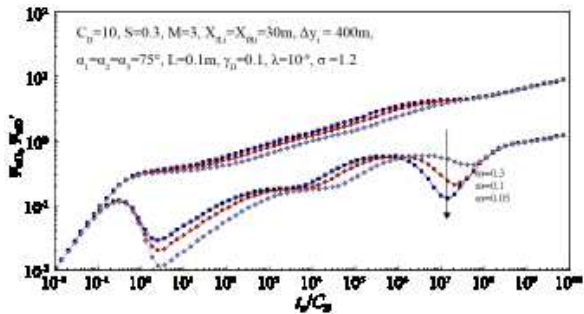


Fig. 4. the effect of elastic storage ratio ω on typical curve

Fig.5 is the effect of the adsorption index σ on the typical curve. As it can be seen from the Fig, when the σ is much smaller, the depression is much shallower.

Fig.6 is the effect of the channeling coefficient λ on the typical curve. As it can be seen from the Fig.6, when the λ is much smaller, the time of the depression occurs is much later.

Fig.7 is the effect of the artificial fracture half-length X_{fi} on the typical curve. As it can be seen from the Fig, the X_{fi} is much smaller, the position of the initial linear flow section is much higher, the initial linear flow section lasts much longer, corresponding, the time of the initial radial flow occurs much later, the duration time is much shorter.

Fig.8 is the effect of the artificial fracture spacing Δy_i on the typical curve. As it

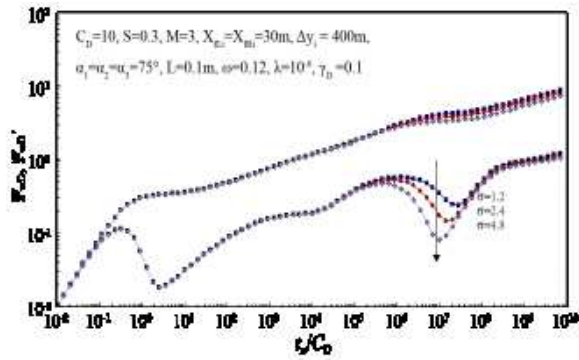


Fig. 5. effect of adsorption index σ on typical curve

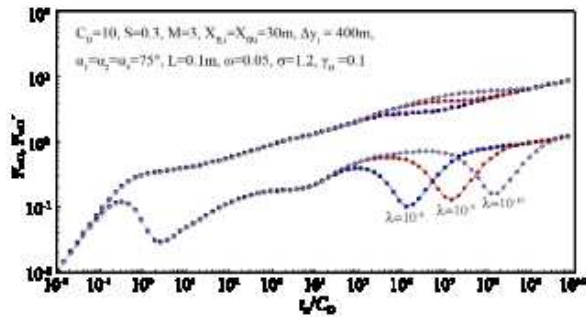


Fig. 6. effect of channeling coefficient λ on typical curve

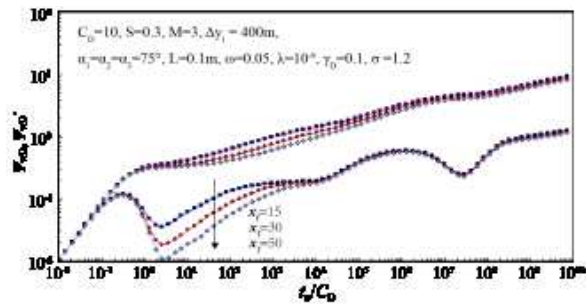


Fig. 7. effect of artificial fracture half-length X_{fi} on typical curve

can be seen from the Fig, the Δ_{yi} is much longer, the initial radial flow section is much more obvious, the time lasts much longer, on the contrary, the Δ_{yi} is much shorter, the initial radial flow section is much shorter, while the Δ_{yi} is small to a certain extent, the initial radial flow section will disappear.

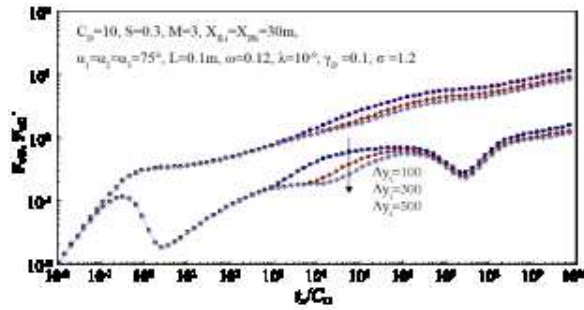


Fig. 8. effect of the artificial fracture spacing Δy_i on the typical curve

6.3. Conclusions

(1) The model not only takes into account the multiple migration mechanism of shale gas (adsorption desorption, diffusion, Darcy percolation), it will also feature the stress sensitive characteristics of deep shale gas at the same time, the well test interpretation model of horizontal well based on multiple mechanisms is established, a well test interpretation of types of multi-stage fracturing horizontal wells for shale gas reservoirs can be obtained.

(2) The whole seepage process of the multi-stage fracturing horizontal well of the shale gas reservoir may appear following feature sections: Early pure wellbore storage section; The first linear flow section; The initial quasi-radial flow section; The second linear flow section; ??Gas diffusion section; The second quasi-radial flow section

(3) The artificial fracture spacing δy_i is much longer, the initial radial

Flow section is much more obvious, and the time of this section lasts much longer.

(4) When the σ is much smaller, the depression is much shallower.

(5) The artificial fracture half-length X_{fi} is much smaller, the position of the initial linear flow section is much higher, and the initial linear flow section lasts much longer.

(6) When production is relatively stable, for the same fracturing fracture, the flow velocity at the fracture tip is greater than that in the middle of the fracture; for the different fracturing fractures, the flow velocity at the end of fracturing horizontal wellbore is greater than that in the middle of fracturing horizontal wellbore fractures.

(7) When the horizontal wells are staged fractured, the fracture layout, which is dense at two ends and thin in the middle in the entire horizontal section can be used.

References

- [1] F. KUCUK: *Transient Flow in Naturally Fractured Reservoirs and Its Application to Devonian Gas Shales*. 55th Annual Fall Technical Conference and Exhibition of the Society of Petroleum Engineers of AIME, 21-24 September, 1980.
- [2] V. A. KUUSKRAA, K. SEDWICK, LEWIN, ET AL: *Technically Recoverable Devonian Shale Gas in Ohio, West Virginia and Kentucky*. The SPE 1985 Eastern Regional Meeting, 6-8 November, 1985.

- [3] E. OZKAN, M. L. BROWN, R. RAGHAVAN, ET AL: *Comparison of fractured-horizontal-well performance in tight sand and shale reservoirs*. SPE Reservoir Evaluation & Engineering 14 (2011), No. 2, 248–259.
- [4] M. BROWN, E. OZKAN, R. RAGHAVAN, H. KAZEMI: *Practical Solutions for Pressure Transient Responses of Fractured Horizontal Wells in Unconventional Reservoirs*. The SPE Annual Technical Conference and Exhibition, 4-7 October, 2009, New Orleans.
- [5] E. OZKAN, R. RAGHAVAN: *Modeling of Fluid Transfer from Shale Matrix to Fracture Network*. The SPE Annual Technical Conference and Exhibition, 19-22 September, 2010, Florence.
- [6] Y. S. WU, M. GEORGE, B. J. BAI: *A Multi-continuum Model for Gas Production in Tight Fracture Reservoirs*. The SPE Hydraulic Fracturing Technology Conference, 19-21 January, 2009, The Woodlands.
- [7] O. RASHEED, BELLO, A. ROBERT: *Multi-stage Hydraulically Fractured Horizontal Shale Gas Well Rate Transient Analysis*. The North Africa Technical Conference and Exhibition, 14-17 February, 2010, Cairo.
- [8] S. ORKHAN, A. A. HASAN: *A New Method for History Matching and Forecasting Shale Gas Reservoir Production Performance with a Dual Porosity Model*. SPE144335 (2011) 1–15.
- [9] M. HAN, G. M. LI, J. Y. CHEN: *Assimilating Microseismic and Welltest Data Using EnKF for Accurate Reservoir Characterisation*. Society of Petroleum Engineers, SPE Journal 20 (2014), No. 1.
- [10] B. HASSAN, S. JAMAL: *Interpretation of Reservoir Flow Regimes and Analysis of Welltest Data in Hydraulically Fractured Unconventional Oil and Gas Reservoirs*. SPE Unconventional Gas Conference and Exhibition, 28-30 January, 2013. Muscat, Oman.
- [11] H. HAMIDREZA, J. MAHMOUD, W. M. PATRICK, CORBETT: *Modeling the Interfering Effects of Gas Condensate and Geological Heterogeneities on Transient Pressure Response*. Society of Petroleum Engineers 18 (2013), No. 4, 656–669.
- [12] N. SIAVASH, Y. JULIANA, LEUNG, V. CLAUDIO: *Integrated Characterization of Hydraulically Fractured Shale-Gas Reservoirs-Production History Matching*. SPE Reservoir Evaluation & Engineering 18 (2015), No. 4, 481–494.

Received November 16, 2016

